JOC*Article*

Isolation and Characterization of Phenyl Viologen as a Radical Cation and Neutral Molecule

William W. Porter, III and Thomas P. Vaid*

Center for Materials Innovation and Department of Chemistry, Washington University, St. Louis, Missouri 63130

vaid@wustl.edu

Received February 21, 2005

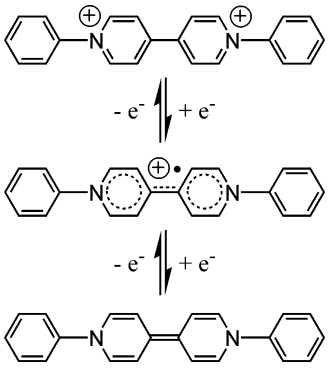

The chemical synthesis, isolation, and characterization of phenyl viologen (PV) as a dication, radical cation, and neutral species are described. Single-crystal X-ray diffraction of $PV^{2+}2Cl^{-}\cdot 2H_2O$ and $PV^{\bullet+}PF_6^{-}\cdot$pyridine reveals the expected differences in bond lengths and also a structural change from two coplanar central rings in $PV^{\bullet+}$ to a twist of 36° between the two central rings in PV^{2+}. The phenyl viologen radical cation exhibits behavior characteristic of many radical cations, including weak π-dimerization in the solid state and reversible π-dimerization in solution. Electrical conductivity measurements of neutral phenyl viologen, the first such measurements of a neutral viologen, reveal that it is a significantly better conductor than the radical cation. Differences in geometric relaxation during charge transfer offer a possible explanation for the higher conductivity of the neutral viologen.

Introduction

The viologens[1] (1,1′-disubstituted 4,4′-bipyridylium dications, Figure 1) are a well-known class of redox couples that undergo two reversible, one-electron reductions to a radical cation and the neutral form.[2] Many of the 1,1′-dialkyl-substituted versions are commercially available as the dications and have been used extensively in electrochemical experiments. Viologens have been thoroughly examined in the solid state as electrochromic materials[3] and more recently as components of supramolecular systems in the solution phase, solid state, and on surfaces.[4]

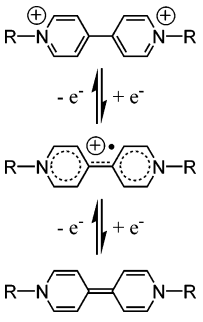

FIGURE 1. Viologens in their dication, radical cation, and neutral form. In phenyl viologen, R = phenyl.

Viologen radical cations have been produced by chemical or electrochemical reduction, photolysis,[5] and even sublimation[6] of viologen dications. Most of the characterization of viologen radical cations has been spectro-

* To whom correspondence should be addressed. Phone: 314-935-8243. Fax: 314-935-4481.

(1) Monk, P. M. S. *The Viologens*; John Wiley and Sons: New York, 1998.

(2) Bird, C. L.; Kuhn, A. T. *Chem. Soc. Rev.* **1981**, *10*, 49−82.

(3) Monk, P. M. S.; Mortimer, R. J.; Rosseinsky, D. R. *Electrochromism: Fundamentals and Applications*; VCH: Weinheim, 1995.

10.1021/jo050328g CCC: $30.25 © 2005 American Chemical Society
Published on Web 05/20/2005

scopic: only the methyl viologen radical cation has been crystallographically characterized.[7] Several of the alkyl viologen radical cations have been studied by ESR,[5,8−12] UV−vis,[7,8] and IR[6,7,13] spectroscopy. Many of those investigations addressed the reversible π-dimerization of the radical cations in solution. ESR and ENDOR investigations of aryl viologens have addressed both the interpretation of the spectra[12,14] and the thermodynamics of the monomer−dimer equilibrium.[15,16] A variety of organic π-radicals are known to undergo a reversible π-dimerization in solution.[17]

The radical cations of viologens, because they are odd-electron species, might be expected to be good electrical conductors as solid, crystalline materials. Several salts of viologens with the 7,7,8,8-tetracyanoquinodimethanide (TCNQ) anion have been synthesized and their solid-state electrical conductivity measured,[18−20] but the oxidation state of the viologen in these compounds is probably best considered to be close to 2^+, although the oxidation state is somewhat ambiguous because TCNQ can exist in either the anionic or neutral form. In any case, the majority of the conductivity in these compounds is likely due to the TCNQ, as indicated by the fact that the conductivity is highest when the TCNQ molecules are present as infinite stacks and are of mixed valence. Viologen radical cations with a well-defined oxidation state (in other words, salts of an anion with a well-defined charge) have rarely been isolated in the solid state. Solid-state conductivity measurements of only one well-defined viologen radical cation, 1,1′-bis(*p*-cyanophenyl)-4,4′-bipyridylium (as the Cl^-, Br^-, BF_4^-, and ClO_4^- salts), have been reported.[21]

The neutral form of the viologens has been investigated to a much smaller extent; the only neutral viologen that has been isolated and characterized is methyl viologen.[7,22] No electrical conductivity measurements of any neutral viologen have been reported.

In the course of our studies of isostructural dopants for molecular semiconductors,[23] we have investigated the neutral form of phenyl viologen as an isostructural n-dopant for *p*-quaterphenyl. Herein we report the synthesis, isolation, and characterization of both neutral phenyl viologen and its radical cation, including the X-ray crystal structure of both the phenyl viologen dication and radical cation and solid-state electrical conductivity measurements of neutral phenyl viologen and the phenyl viologen radical cation.

Experimental Section

General Procedures and Materials. All manipulations were carried out using Schlenk line or glovebox techniques unless otherwise noted. Reagents were purchased from commercial suppliers and purified and dried by the following methods. Aniline was distilled twice prior to use, tetrabutylammonium hexafluorophosphate was recrystallized twice from ethanol, and *p*-quaterphenyl was recrystallized from xylene. Acetonitrile was distilled from phosphorus pentoxide and vacuum transferred from activated 3 Å molecular sieves immediately prior to use. Dimethyl sulfoxide was distilled from sodium hydroxide and stored over activated 3 Å molecular sieves. Absolute ethanol was distilled from Mg/I_2 and vacuum transferred from 3 Å molecular sieves immediately prior to use. Dimethyl sulfoxide-d_6 was dried over 3 Å molecular sieves and stored in a nitrogen-filled glovebox. Acetonitrile-d_3 was vacuum transferred onto 3 Å molecular sieves from phosphorus pentoxide and stored in a nitrogen-filled glovebox. Xylene and hexane were distilled from a purple sodium benzophenone solution with added tetraglyme. Pyridine was distilled from potassium hydroxide and vacuum transferred from 3 Å molecular sieves immediately prior to use.

^{1}H NMR (300 MHz) and ^{13}C NMR (75 MHz) spectra were recorded as solutions in the solvents as noted below. Infrared spectra were obtained as Nujol mulls (made with a small mortar and pestle) on NaCl plates. The ESR spectrum was obtained on an X-band spectrometer with 0.10 G modulation.

1,1′-Diphenyl-4,4′-bipyridinium dichloride ($PV^{2+}2Cl^-$) was prepared by a published procedure;[24] the intermediate 1,1′-bis(2,4-dinitrophenyl)-4,4′-bipyridiinium dichloride was recrystallized from acetone/water. Data for orange $PV^{2+}2Cl^-$. Mp: 306−308 °C (under N_2, dec). ^{1}H NMR (DMSO-d_6, ref DMSO-d_5 at 2.50 ppm): δ 9.76 (d, 4H, J = 6.9 Hz), 9.16 (d, 4H, J = 6.9 Hz), 8.01 (m, 4H), 7.81 (m, 6H). ^{13}C NMR (DMSO-d_6, ref DMSO-d_6 at 39.51 ppm): δ 148.9, 146.0, 142.3, 131.6, 130.3, 126.8, 124.9. UV−vis (DMSO, 5.8×10^{-5} M): λ_{max} = 314 nm, $\epsilon = 2.1 \times 10^4$ L·mol^{-1}·cm^{-1}. IR (Nujol, cm^{-1}): 1628 (m), 1242 (w), 1032 (vw), 998 (vw), 854 (w), 764 (s), 691 (m).

1,1′-Diphenyl-4,4′-bipyridinium Bis(hexafluorophosphate) ($PV^{2+}2PF_6^-$). $PV^{2+}2Cl^-$ (1.175 g, 3.08 mmol) was dissolved in a minimal amount of hot H_2O. A solution of NH_4PF_6 (6.143 g, 37.7 mmol) in 15 mL of H_2O was added. The resulting pale yellow precipitate was collected via filtration and recrystallized from ethanol/water to give 1.791 g (96%) of orange crystals.

Neutral Phenyl Viologen (PV^0). Ethanol (50 mL), $PV^{2+}2Cl^-$ (1.181 g, 3.10 mmol), and zinc dust (0.801 g, 12.2 mmol) were combined in a 100-mL flask, and the stirred suspension was brought to reflux under N_2 for 96 h. The resulting slurry was cooled to room temperature, filtered, and washed with ethanol. The mixture of an insoluble red product and excess zinc was dried under vacuum and separated by

(4) Jang, S. S.; Jang, Y. H.; Kim, Y.-H.; Goddard, W. A. I.; Flood, A. H.; Laursen, B. W.; Tseng, H.-R.; Stoddart, J. F.; Jeppesen, J. O.; Choi, J. W.; Steuerman, D. W.; DeIonno, E.; Heath, J. R. *J. Am. Chem. Soc.* **2005**, *127*, 1563−1575 (and references therein).
(5) Johnson, C. S.; Gutowsky, H. S. *J. Chem. Phys.* **1963**, *39*, 58−62.
(6) Poizat, O.; Sourisseau, C.; Mathey, Y. *J. Chem. Soc., Faraday Trans. 1* **1984**, *80*, 3257−3274.
(7) Bockman, T. M.; Kochi, J. K. *J. Org. Chem.* **1990**, *55*, 4127−4135.
(8) Kosower, E. M.; Cotter, J. L. *J. Am. Chem. Soc.* **1964**, *86*, 5524−5527.
(9) Evans, A. G.; Evans, J. C.; Baker, M. W. *J. Am. Chem. Soc.* **1977**, *99*, 5882−5884.
(10) Evans, A. G.; Evans, J. C.; Baker, M. W. *J. Chem. Soc., Perkin Trans. 2* **1977**, 1787−1789.
(11) Guerin-Ouler, D.; Nicollin, C.; Sieiro, C.; Lamy, C. *Mol. Phys.* **1977**, *34*, 161−170.
(12) Clack, D. W.; Evans, J. C.; Obaid, A. Y.; Rowlands, C. C. *Tetrahedron* **1983**, *39*, 3615−3620.
(13) Hester, R. E.; Suzuki, S. *J. Phys. Chem.* **1982**, *86*, 4626−4630.
(14) Clack, D. W.; Evans, J. C.; Obaid, A. Y.; Rowlands, C. C. *J. Chem. Soc., Perkin Trans. 2* **1985**, 1653−1657.
(15) Evans, J. C.; Nouri-Sorkhabi, M. H.; Rowlands, C. C. *Tetrahedron* **1982**, *38*, 2581−2584.
(16) Evans, J. C.; Evans, A. G.; Nouri-Sorkhabi, N. H.; Obaid, A. Y.; Rowlands, C. C. *J. Chem. Soc., Perkin Trans. 2* **1985**, 315−318.
(17) Lü, J.-M.; Rosokha, S. V.; Kochi, J. K. *J. Am. Chem. Soc.* **2003**, *125*, 12161−12171.
(18) Ashwell, G. J.; Allen, J. G. *J. Phys.* **1983**, *44* (C3), 1261−1264.
(19) Ashwell, G. J.; Allen, J. G.; Goodings, E. P.; Nowell, I. W. *Phys. Status Solidi A* **1984**, *82*, 301−306.
(20) Ashwell, G. J.; Cross, G. H.; Kennedy, D. A.; Nowell, I. W.; Allan, J. G. *J. Chem. Soc., Perkin Trans. 2* **1983**, 1787−1791.
(21) Rosseinsky, D. R.; Monk, P. M. S. *J. Chem. Soc., Faraday Trans.* **1994**, *90*, 1127−1131.
(22) Mohammad, M. *J. Org. Chem.* **1987**, *52*, 2779−2782.
(23) Vaid, T. P.; Lytton-Jean, A. K.; Barnes, B. C. *Chem. Mater.* **2003**, *15*, 4292−4299.
(24) Kamogawa, H.; Sato, S. *Bull. Chem. Soc. Jpn.* **1991**, *64*, 321−323.

sublimation under high vacuum at 250 °C for 50 h to yield 0.670 g (70%) of red PV^0. Mp: 359−361 °C. ^{1}H NMR (DMSO-d_6, 90 °C): δ 7.34 (t, 4H, J = 7.8 Hz), 7.17 (d, 4H, J = 7.8 Hz), 7.02 (t, 2H, J = 7.3 Hz), 6.60 (d, 4H, J = 8.2 Hz), 5.78 (d, 4H, J = 8.2 Hz). ^{13}C NMR (DMSO-d_6, 90 °C, partial spectrum): δ 129.1, 125.4, 121.9, 116.2, 109.0. UV−vis in THF, saturated: λ_{max} = 442 nm; 462 nm (overlapping peaks, fit to two Gaussian peaks). IR (Nujol, cm^{-1}): 1660 (m), 1609 (w), 1554 (w), 1519 (m), 1306 (s), 1232 (w), 1019 (w), 984 (m), 805 (m), 744 (m). HREI MS: $C_{22}H_{18}N_2$ 310.147 calculated, 310.148 found. Anal. Calcd for $C_{22}H_{18}N_2$: C, 85.13; H, 5.35; N, 9.02. Found: C, 85.45; H, 5.35; N, 8.83.

Phenyl Viologen Radical Cation Hexafluorophosphate ($PV^{\bullet+}PF_6^-$). A mixture of $PV^{2+}2PF_6^-$ (188 mg, 0.313 mmol) and PV^0 (97 mg, 0.313 mmol) in 15 mL of acetonitrile was brought to reflux under N_2 for 16 h. After cooling of the dark green solution to room temperature, the acetonitrile was slowly removed under vacuum to give 0.268 g (96%) of dark purple microcrystals. UV−vis (CH_3CN, 4.5 × 10^{-5} M) nm, ϵ (L·mol^{-1}·cm^{-1}) (many overlapping peaks; fit to a set of Gaussian peaks): 250, 5.4 × 10^3; 318, 3.7 × 10^3; 377, 4.2 × 10^3; 437, 2.4 × 10^4; 627, 1.1 × 10^4; 644, 2.2 × 10^3; 664, 3.7 × 10^3; 713, 7.3 × 10^3. IR (Nujol, cm^{-1}): 1634 (s), 1587 (m), 1572 (m), 1509 (w), 1489 (s), 1343 (w), 1266 (s), 1197 (s), 1022 (m), 1015 (m), 985 (w), 843 (s), 759 (m), 695 (w), 604 (w), 557 (w).

Cocrystallization of *p*-Quaterphenyl and PV^0. A mixture of 197 mg of *p*-quaterphenyl, 20 mg of PV^0, and 90 mL of *p*-xylene was heated to 135 °C to form a pale red solution. The solution was allowed to cool to room temperature with stirring over a period of 4 h. Metallic red plates were collected by filtration, washed with three 20-mL portions of ether, and dried under vacuum at 50 °C. Isolated yield: 160 mg.

Magnetic Susceptibility of $PV^{\bullet+}PF_6^-$. Solution-phase susceptibility was measured as a solution in CD_3CN by the Evans method as described previously.[23] Solid-state susceptibility measurements were performed at room temperature with a Johnson Matthey Mark I magnetic susceptibility balance.

Electrochemistry and Solid-State Conductivity. Cyclic voltammetry and solid-state conductivity measurements were performed with an EG&G/PAR 263A potentiostat with electrical connection to the inside of a nitrogen-filled drybox, where all materials and solutions were maintained during the measurements. Cyclic voltammetry was performed on saturated solutions of the analyte in anhydrous THF with 0.10 M [Bu_4N][PF_6] supporting electrolyte and 0.0013 M ferrocene internal standard. Scans were run at a rate of 50 mV/s with a 5.3 Hz low-pass filter. The working and pseudoreference electrodes were 0.50 mm diameter platinum disks and the counter electrode was a 2.5 mm diameter platinum disk. Solid-state conductivity of pressed powders was measured in a two-electrode configuration on a home-built apparatus that consists of a Delrin block with a 6.35 mm diameter cylindrical hole and two 6.35 mm diameter copper cylindrical contacts. The material to be studied was inserted between the two contacts within the Delrin block and a mass of 3.85 kg was placed on the top contact, thus applying 12 bar pressure.

X-ray Crystallography. Without the exclusion of air or water, orange prisms of $PV^{2+}2Cl^-\cdot 2H_2O$ were grown by cooling a hot solution in 1:1 ethyl acetate/acetone. Purple needles of $PV^{\bullet+}PF_6^-\cdot$(pyridine) were grown by slow diffusion of hexane into a pyridine solution. Data collection was performed at the University of Houston on a Siemens SMART platform diffractometer equipped with a 1 K CCD area detector. Crystals were mounted in mineral oil and data were collected at 223 K. An empirical absorption correction was applied. Structures were solved with SHELXS and refined with SHELXL.

Attempted Crystal Structure of PV^0. Crystals of PV^0 grown by slow sublimation under vacuum diffracted X-rays well. However, in all attempts the crystals were conglomerates and a single-crystal structure was unattainable. Crystals of PV^0 grown by controlled cooling of a *p*-xylene solution also diffracted X-rays. However, in this case the crystals were large plates that were too thin to obtain a structure.

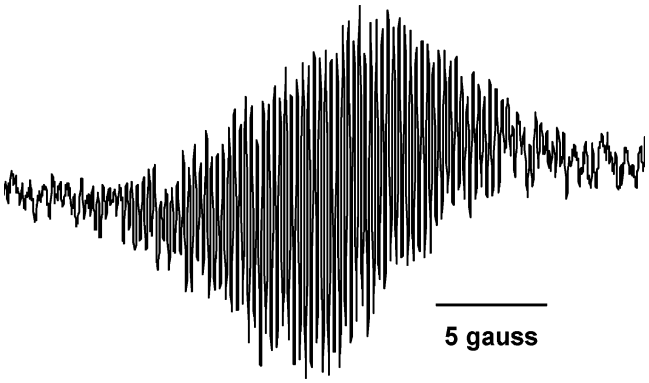

FIGURE 2. ESR spectrum of $PV^{\bullet+}PF_6^-$ in THF.

Results and Discussion

Synthesis. 1,1′-Diphenyl-4,4′-bipyridinium dichloride ($PV^{2+}2Cl^-$) was prepared by a published procedure.[24] Reduction of $PV^{2+}2Cl^-$ by zinc in ethanol gave neutral phenyl viologen (PV^0), which has very little solubility in any solvent. Sublimation of PV^0 under vacuum at 250 °C yielded red, thin, plate-shaped crystals of PV^0. Because $PV^{2+}2Cl^-$ has poor solubility in most organic solvents, it was converted to the hexafluorophosphate ($PV^{2+}2PF_6^-$) by precipitation from an aqueous solution by addition of a solution of NH_4PF_6. The phenyl viologen radical cation hexafluorophosphate, $PV^{\bullet+}PF_6^-$, was prepared by conproportionation of $PV^{2+}2PF_6^-$ and PV^0 in acetonitrile. The radical cation forms a deep green solution in acetonitrile but is dark purple in the solid state.

Spectroscopy. UV−vis spectra of PV^0 and $PV^{\bullet+}PF_6^-$ in THF and CH_3CN, respectively, were similar to reported spectra of the analogous methyl viologen compounds, MV^0 and $MV^{\bullet+}PF_6^-$.[7] Because there were overlapping peaks in each spectrum, they were both fit to sets of Gaussian peaks to obtain the wavelengths and absorptivities reported in the Experimental Section.

An ESR spectrum of a dilute solution of $PV^{\bullet+}PF_6^-$ in THF (Figure 2) consists of a series of lines spaced by approximately 0.266 G (determined by Fourier transform of the spectrum), in agreement with a simulated spectrum produced with published hyperfine couplings.[12]

Crystal Structures of $PV^{2+}2Cl^-\cdot 2H_2O$ and $PV^{\bullet+}PF_6^-\cdot$Pyridine. Crystallographic data for $PV^{2+}2Cl^-\cdot 2H_2O$ and $PV^{\bullet+}PF_6^-\cdot$pyridine and CIF files are provided in the Supporting Information. The structure of $PV^{2+}2Cl^-\cdot 2H_2O$ consists of stacks of PV^{2+} cations with well-separated Cl^- anions. The two chlorides and two waters of crystallization form a hydrogen-bonded square with chlorides and water molecules at alternate corners, each water donating two hydrogens and each chloride accepting two. Crystals of $PV^{\bullet+}PF_6^-\cdot$pyridine consist of infinite stacks of $PV^{\bullet+}$ radical cations and separate columns of partly disordered PF_6^- anions with one partly disordered pyridine of crystallization per formula unit.

Figure 3 shows the solid-state structures of PV^{2+} in $PV^{2+}2Cl^-\cdot 2H_2O$ (top) and $PV^{\bullet+}$ in $PV^{\bullet+}PF_6^-\cdot$pyridine

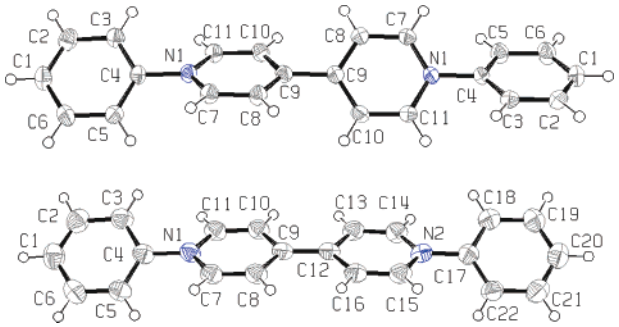

FIGURE 3. Solid-state structure of PV^{2+} in $PV^{2+}2Cl^{-}\cdot 2H_2O$ (top) and $PV^{\bullet+}$ in $PV^{\bullet+}PF_6^{-}\cdot$pyridine (bottom).

TABLE 1. Representative Dihedral Angles in PV^{2+} and $PV^{\bullet+}$

	angle (deg)	
dihedral	PV^{2+}	$PV^{\bullet+}$
C(3)−C(4)−N(1)−C(11)	37.4(2)	32.0(4)
C(10)−C(9)−C(9)−C(8)	37.7	1.0(5)
C(10)−C(9)−C(12)−C(13)		
C(11)−N(1)−C(4)−C(3)	37.4(2)	33.4(4)
C(15)−N(2)−C(17)−C(22)		

(bottom). The most obvious difference between the two structures is the alternating twist in the planes of the aromatic rings that is present between all the rings in PV^{2+}, whereas in $PV^{\bullet+}$ the two central rings are nearly coplanar. Table 1 lists the dihedral angles for representative sets of atoms in the two ions. In PV^{2+}, the inter-ring twists are consistently near 37°. For $PV^{\bullet+}$, the dihedral angles between the outer phenyl groups and the viologen core are about 33°, while the two central rings are nearly coplanar with a twist of 1°. The driving force for the observed twists between rings is the steric interaction between hydrogens on the ortho carbons of adjacent rings. A low-temperature crystal structure of *p*-quaterphenyl, which is isoelectronic with PV^{2+}, indicates similar inter-ring twists of 17−22°,[25] although there is significant torsional motion in the crystals at room temperature.[26] The coplanarity of the two central rings of $PV^{\bullet+}$ is due to conjugation between the rings, as illustrated in Figure 1. The bond order of the C(9)−C(12) bond is approximately 1.5, and twisting the two central rings relative to each other would break the partial π-bond. The published crystal structure of the methyl viologen radical cation contains two independent cations with inter-ring torsional angles of 7° and 11°,[7] somewhat larger than might have been expected.

The bond lengths of PV^{2+} and $PV^{\bullet+}$ are given in Table 2. There are some slight, insignificant differences in the carbon−carbon bond lengths of the phenyl groups of the two cations. The inner two rings of the two cations, on the other hand, display the expected variations in bond lengths due to their different electronic structures. In PV^{2+}, the two central rings are aromatic and the bond lengths are similar to those in previously reported viologen dications. In $PV^{\bullet+}$ the bonds C(7)−C(8), C(10)−C(11), and C(9)−C(12) have decreased in length (relative to PV^{2+}) and the bonds C(7)−N(1), C(11)−N(1), C(8)−C(9), and C(9)−C(10) have increased in length, as expected for a molecule with a valence-bond representation that is halfway between that of the aromatic dication and the quinoid neutral viologen (see Figure 1). The most pronounced change is seen at the central C(9)−C(12) bond, where the difference in bond length is 0.057 Å.

TABLE 2. Representative Bond Lengths in PV^{2+} and $PV^{\bullet+}$

	distance (Å)			distance (Å)	
bond	PV^{2+}	$PV^{\bullet+}$	bond	PV^{2+}	$PV^{\bullet+}$
C(1)−C(2)	1.386(2)	1.374(5)	C(7)−C(8)	1.3755(19)	1.348(4)
C(2)−C(3)	1.386(2)	1.380(5)	C(8)−C(9)	1.391(2)	1.422(4)
C(3)−C(4)	1.383(2)	1.388(5)	C(9)−C(10)	1.396(2)	1.424(4)
C(4)−C(5)	1.388(2)	1.384(4)	C(10)−C(11)	1.374(2)	1.349(4)
C(5)−C(6)	1.385(2)	1.385(5)	C(11)−N(1)	1.3590(18)	1.375(4)
C(6)−C(1)	1.380(2)	1.382(5)	C(9)−C(9)	1.485(3)	1.427(4)
C(4)−N(1)	1.4580(17)	1.438(4)	C(9)−C(12)		
N(1)−C(7)	1.3520(18)	1.375(4)			

There are hundreds of published X-ray crystal structures containing 1,1′-dialkyl viologen dications, most commonly as methyl viologen salts or as dialkyl viologens that are part of a larger supramolecular system. Surprisingly, in the majority of the dications the two aromatic rings appear to be coplanar. It is possible that in many cases the apparent coplanarity of the rings is due to a dynamic solid-state structure in which the rings are twisting relative to each other, with two energy minima on either side of the coplanar structure, resulting in an averaged X-ray structure that appears to have coplanar rings. This phenomenon has been thoroughly studied in crystals of biphenyl.[27,28]

It is also possible that in many of the viologen dications the rings are in fact coplanar and static in that configuration. Partial charge transfer from the counteranions to the viologen dications, resulting in some contribution of the radical cation electronic structure in the dications, could provide the driving force for adoption of the coplanar structure. For example, in the methyl viologen dihalides (dichloride, dibromide, and diiodide) the viologen dications are planar.[29] There are close contacts between the halide anions and the methyl viologen cations in each of the crystals, and there is spectroscopic evidence for a charge-transfer interaction, at least in the cases of the iodide and bromide.[30] Another interesting set of methyl viologen salts occur with $CoCl_4^{2-}$, $[CuCl_2]_n^{n-}$, and $PdCl_4^{2-}$ as the anions. In the two salts in which there is evidence of charge transfer,[30] $CoCl_4^{2-}$ and $[CuCl_2]_n^{n-}$, the methyl viologen ions are planar.[31] In the $PdCl_4^{2-}$ salt, where there is no evidence of charge transfer and the cation and anion are well separated, the methyl viologen cation's two rings are twisted 50° relative to each other. The authors attribute the differences in structure to crystal packing effects,[31] but the distinct difference in

(25) Baudour, J. L.; Delugeard, Y.; Rivet, P. *Acta Crystallogr. B* **1978**, *B34*, 625−628.
(26) Delugeard, Y.; Desuche, J.; Baudour, J. L. *Acta Crystallogr. B* **1976**, *32*, 702−705.
(27) Cailleau, H.; Baudour, J. L.; Zeyen, C. M. E. *Acta Crystallogr.* **1979**, *B35*, 426−432.
(28) Corish, J.; Morton-Blake, D. A.; O'Donoghue, F.; Baudour, J. L.; Beniere, F.; Toudic, B. *Theochem* **1995**, *358*, 29−38.
(29) Russell, J. H.; Wallwork, S. C. *Acta Crystallogr. B* **1972**, *B28*, 1527−1533.
(30) Macfarlane, A. J.; Williams, R. J. P. *J. Chem. Soc. (A)* **1969**, 1517−1520.
(31) Prout, C. K.; Murray-Rust, P. *J. Chem. Soc. (A)* **1969**, 1520−1525.

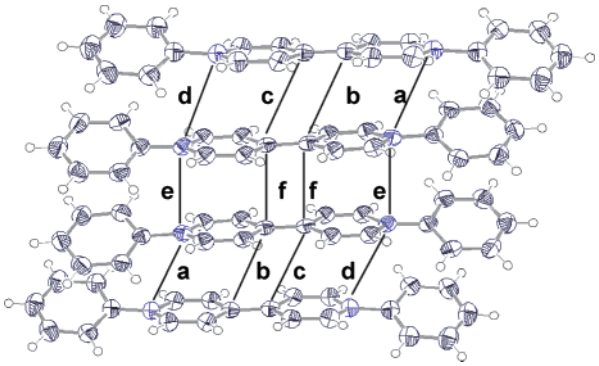

FIGURE 4. Stacking of $PV^{\bullet+}$ radical cations in $PV^{\bullet+}PF_6^-\cdot$ pyridine. Distances are as follows (in Å): $a = 3.973$, $b = 4.003$, $c = 3.955$, $d = 3.852$, $e = 3.502$, $f = 3.339$.

structure between our PV^{2+} dication and $PV^{\bullet+}$ radical cation lend credence to the idea that electronic effects may be important.

There are two published structures of 1,1′-diaryl viologen dications (the *p*-fluorophenyl[19] and *p*-cyanophenyl[20] derivatives), and in both structures the viologen cation has two coplanar central rings and two outer rings that are twisted relative to the central rings. In both compounds $TCNQ^-$ is the counterion, so it is likely that the charge on the cations is not a full 2+, resulting in the observed structures.

The structure of $PV^{\bullet+}PF_6^-\cdot$pyridine exhibits one other notable feature: the stacks of $PV^{\bullet+}$ consist of pairs of closely spaced radical cations. Figure 4 shows four radical cations with labeled interatomic distances. The closest intermolecular contact, labeled *f*, is 3.34 Å between two central carbons. The intermolecular distance between nitrogens on the same two molecules is 3.50 Å, indicating some bending of the radical cations. A contact of 3.34 Å is at the high end of the range of distances of shortest contact observed in π-dimers in the solid state.[17] Still, the dimerization might lead to some spin pairing and a paramagnetic susceptibility less than that expected from one unpaired electron per radical cation, so the magnetic susceptibility of $PV^{\bullet+}PF_6^-\cdot$pyridine was examined in the solid state and in solution.

Magnetic Susceptibility.

(i) Solid State. Our intent was to examine the solid-state properties of $PV^{\bullet+}PF_6^-\cdot$pyridine so that a correlation between its solid-state properties and the observed X-ray structure could be examined, but we found it difficult to isolate $PV^{\bullet+}PF_6^-\cdot$pyridine with a full equivalent of pyridine in the crystals. Oxidation of samples of $PV^{\bullet+}PF_6^-\cdot(\text{pyridine})_x$ with I_2 in DMSO-d_6 to the dication and integration of the ^{1}H NMR spectrum revealed that a sample that had been under vacuum had the stoichiometry $PV^{\bullet+}PF_6^-\cdot(\text{pyridine})_{0.12}$. However, this sample was still visibly crystalline and had a powder X-ray diffraction pattern in reasonable agreement with a powder pattern simulated with the single-crystal data of $PV^{\bullet+}PF_6^-\cdot(\text{pyridine})_{1.0}$. Therefore, it is likely that the relevant infinite stacks of $PV^{\bullet+}$ are maintained in $PV^{\bullet+}PF_6^-\cdot(\text{pyridine})_x$ when some pyridine has left the crystals.

The magnetic susceptibility of microcrystalline $PV^{\bullet+}PF_6^-\cdot(\text{pyridine})_{0.12}$ was measured at room temperature on two separate samples. Each sample was shaken and repacked between measurements, and a total of six measurements were taken on each sample. The molar susceptibility was calculated and a correction for diamagnetism[32,33] of 2.72×10^{-4} emu/mol was applied. The magnetic moments calculated from the data of the two samples were 1.55(4) and 1.58(3) μ_B. Both are less than the ideal value of 1.73 μ_B for one unpaired electron, presumably because of spin pairing in the dimers seen in the crystal structure.

TABLE 3. Magnetic Susceptibility of $PV^{\bullet+}PF_6^-$ in CD_3CN Solution Determined by the Evans Method[a]

concn (M)	T (°C)	apparent μ (μ_B)	concn (M)	T (°C)	apparent μ (μ_B)
0.0665	20.6	1.02	0.0397	21.6	1.15
0.0397	21.6	1.15	0.0389	32.0	1.24
0.01976	21.7	1.26	0.0384	42.0	1.29
0.00988	21.0	1.41	0.0379	49.0	1.32
0.00494	20.6	1.58	0.0375	58.0	1.34
0.00247	21.0	1.75			

[a] The left side of the table shows data for a range of concentrations and the right side of the table shows data for a range of temperatures.

(ii) Solution Phase. An Evans method[34] determination of the magnetic susceptibility of $PV^{\bullet+}PF_6^-$ as a solution in CD_3CN indicated a magnetic moment of only about 1.2 μ_B per radical cation, much less than the ideal value of 1.73 μ_B. The reversible π-dimerization of viologen radical cations to diamagnetic dimers has been observed previously in solution,[9,10,15,16] so an investigation of the concentration and temperature dependence of the magnetic moment was undertaken. Table 3 presents the magnetic moment of $PV^{\bullet+}PF_6^-$ in CD_3CN over a range of concentrations and temperatures. At room temperature, concentrations from 0.0665 to 0.00247 M were examined and displayed apparent magnetic moments of 1.02 μ_B to 1.75 μ_B, increasing with decreasing concentration, as expected for a monomer−dimer equilibrium shifting toward monomer. Furthermore, Table 3 shows the increase in apparent magnetic moment as the temperature of a solution is raised from 22 to 58 °C, once again consistent with a shift in the equilibrium from dimer to monomer. (The small decrease in concentration with increasing temperature is due to thermal expansion of the solvent.) The data are not accurate enough to extract thermodynamic parameters for the monomer−dimer equilibrium. It is interesting that in the more concentrated solutions the apparent magnetic moment is lower than it is in the solid state. It is possible that the packing of $PV^{\bullet+}$ in $PV^{\bullet+}PF_6^-\cdot$pyridine is not ideal for π-dimerization and the radical cations are able to find a more favorable orientation in solution.

Solid-State Conductivity of PV^0 and $PV^{\bullet+}PF_6^-\cdot(\text{Pyridine})_{0.43}$. Polycrystalline samples were pressed between two freshly cleaned copper contacts in the apparatus described in the Experimental Section. Because these were simple two-point measurements, a series of sample masses for each substance were measured to examine the influence of contact resistance. The

(32) Carlin, R. L. *Magnetochemistry*; Springer-Verlag: New York, 1986.
(33) Weast, R. C.; Ed. *CRC Handbook of Chemistry and Physics*, 67th ed.; CRC Press: Boca Raton, FL, 1986.
(34) Evans, D. F. *J. Chem. Soc.* **1959**, 2003−2005.

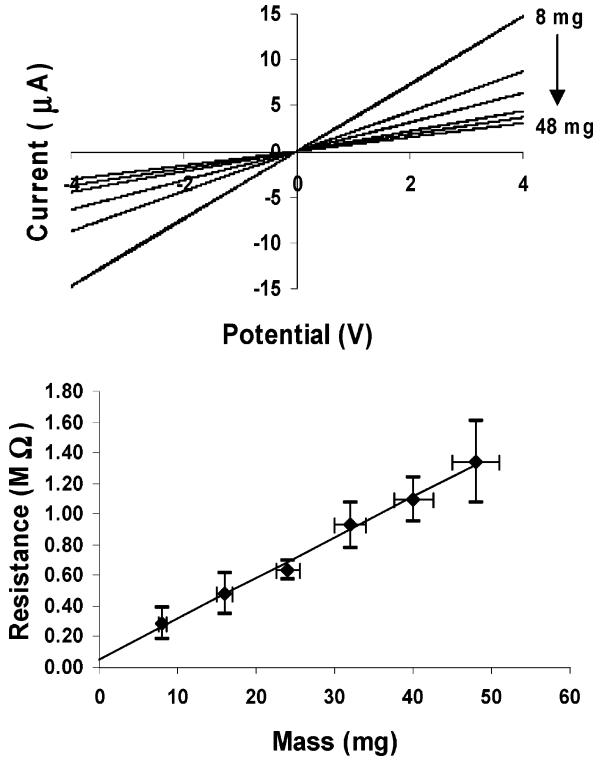

FIGURE 5. Solid-state electrical conductivity measurements of PV^0. The top figure is current−voltage plots for a series of sample masses (8, 16, 24, 32, 40, 48 mg). The bottom figure is the resistance of the samples plotted versus their mass. Extrapolation to zero mass yields the contact resistance of 54 kΩ.

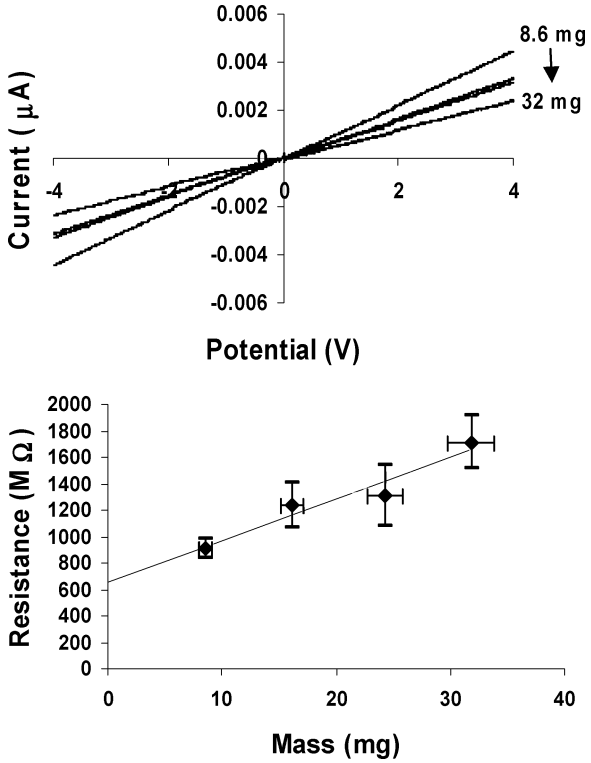

FIGURE 6. Solid-state electrical conductivity measurements of $PV^{\bullet+}PF_6^-\cdot(pyridine)_{0.43}$. The top figure is current−voltage plots for a series of sample masses (8.6, 16.1, 24.3, 31.8 mg). The bottom figure is the resistance of the samples plotted versus their mass. Extrapolation to zero mass yields the contact resistance of 650 MΩ.

cross-sectional area of the pressed pellets in the apparatus is constant, so the thickness of the sample, and therefore its measured resistance, will increase in direct proportion to the sample mass if the contact resistance is not significant. At each mass, the same sample was repacked and measured for a total of four measurements. Current was measured as a function of applied potential from 0 to +4 to −4 to 0 V. Each current−voltage plot in Figures 5 and 6 is the average of the four runs at each mass.

Figure 5 shows the results for PV^0. The current−voltage plots for several masses are shown in the top graph and all of them are linear, indicating Ohmic behavior. The inverse of the slope of each plot (obtained by linear regression) is the resistance. The resistance as a function of mass is shown in the bottom graph. The horizontal error bars represent the estimated weighing error, and the vertical error bars are the standard deviation over the four measurements at each mass (representing, essentially, the variation due to sample packing). Extrapolation of a least-squares-fit line to zero mass yields the contact resistance, which is a relatively small 54 kΩ. The conductivity of PV^0 was calculated by assuming a density of 1.25 g/cm^3 and using the known cross-sectional area of the sample disk (0.317 cm^2) to calculate the sample thickness. The contact resistance of 54 kΩ was subtracted from all measurements. An average conductivity of 3.1×10^{-7} ($\pm 0.6 \times 10^{-7}$) Ω^{-1}cm^{-1} was calculated from 24 measurements (four times each on six samples).

Figure 6 shows the results of conductivity measurements of $PV^{\bullet+}PF_6^-\cdot(pyridine)_{0.43}$. The data were treated in the same manner as those for PV^0. In this case, the contact resistance is significant, 650 MΩ. The density calculated from the crystal structure (1.46 g/cm^3) was used in the calculation of the resistivity. An average conductivity of 2.3×10^{-10} ($\pm 0.7 \times 10^{-10}$) Ω^{-1}cm^{-1} was calculated from 16 measurements. (Similar results were obtained for a sample of $PV^{\bullet+}PF_6^-\cdot(pyridine)_{0.12}$.) There is one previous report of the conductivity of an aryl viologen radical cation: *p*-cyanophenyl viologen radical cation as a pressed powder has a conductivity between 7.1×10^{-9} and 5.0×10^{-7} Ω^{-1}cm^{-1}, depending upon the anion and preparation method.[21] The lower resistivity of that material may be intrinsic but may be due in part to the much higher pressures applied to the samples in those experiments.

It is somewhat surprising that the closed-shell PV^0 has an electrical conductivity 3 orders of magnitude higher than the radical $PV^{\bullet+}PF_6^-\cdot(pyridine)_x$. The difference may be partly due to differences in crystal packing and intermolecular contacts in the solid state. But if charge transport through the crystal occurs by a hopping mechanism, which is most likely the best description of charge transport in these systems, then the geometric transformation that accompanies charge transfer from one molecule to the next is another important factor affecting charge mobility. Both PV^0 and $PV^{\bullet+}$ are easily oxidized species, so in both PV^0 and $PV^{\bullet+}PF_6^-\cdot(pyridine)_x$ the solid-state charge carriers are almost certainly holes. When a

hole moves through a crystal of PV^0, the two species involved in charge transfer are PV^0 and $PV^{\bullet+}$. There is some change in bond lengths between PV^0 and $PV^{\bullet+}$, but the overall molecular structure, with two coplanar central rings and two outer rings twisted relative to those (an assumption for PV^0), is the same. In contrast, the relevant species for charge transport in $PV^{\bullet+}PF_6^-\cdot(\text{pyridine})_x$ are $PV^{\bullet+}$ and PV^{2+}, which have coplanar and twisted central rings, respectively. Charge transport in $PV^{\bullet+}PF_6^-\cdot(\text{pyridine})_x$ therefore involves a major molecular rearrangement with each hop (of course, it may be difficult for PV^{2+} within a crystal of $PV^{\bullet+}PF_6^-\cdot(\text{pyridine})_x$ to actually adopt its preferred geometry). A recent paper reported theoretical calculations that showed that, in molecular conductors, hole mobilities are determined in large part by the reorganization energy that accompanies charge transfer and changes in inter-ring dihedral angles are a significant component of the reorganization energy.[35]

Electrochemistry. Our original motivation for isolating PV^0 was to investigate its behavior as an isostructural n-dopant[23] for *p*-quaterphenyl. One requirement for isostructural n-doping is that the dopant molecule donates an electron to the host organic semiconductor in the solid state. Solution-phase electrochemistry provides an estimate of the electronic energy levels in the solid state. For PV and *p*-quaterphenyl, for example, if the $PV^{0/+}$ potential is negative of the *p*-quaterphenyl$^{0/-}$ potential, then PV^0 should spontaneously transfer an electron to neutral *p*-quaterphenyl in the solution phase and possibly in the solid state. Although the electrochemical reduction potentials of phenyl viologen in water[2] and *p*-quaterphenyl in dimethylamine[36] have been reported, it is necessary to compare their electrochemistry under identical conditions. Cyclic voltammograms of *p*-quaterphenyl and $PV^{2+}2PF_6^-$ in THF with 0.10 M $[Bu_4N][PF_6]$ supporting electrolyte are shown in Figure 7. An internal reference of ferrocene$^{0/+}$ was set to 0 V. Two reversible, one-electron reductions of PV^{2+}occur at −0.68 and −0.94 V. Two reversible, one-electron reductions of *p*-quaterphenyl occur at −2.81 and −2.99 V. In a separate experiment, a nonreversible oxidation of *p*-quaterphenyl was observed at approximately 1.27 V. The combined data indicate that *p*-quaterphenyl has a band gap of approximately 4.1 eV and the donor level of PV^0 in *p*-quaterphenyl lies approximately 1.9 eV from the conduction band edge, so there is little chance that PV^0 will act as a donor in *p*-quaterphenyl. Nevertheless, we examined their cocrystallization and the conductivity of the cocrystals.

Cocrystallization of PV^0 and Quaterphenyl. Slow cooling of a hot *p*-xylene solution of *p*-quaterphenyl yields thin, colorless, plate-shaped crystals. Powder X-ray diffraction agreed with the unit cell of a reported single-crystal structure.[26] Cooling a 9:1 mixture of *p*-quaterphenyl and PV^0 under the same conditions results in thin, red, plate-shaped crystals. Powder diffraction showed that the unit cell was unchanged and no other crystalline phases were present, including crystals of pure PV^0. Thus

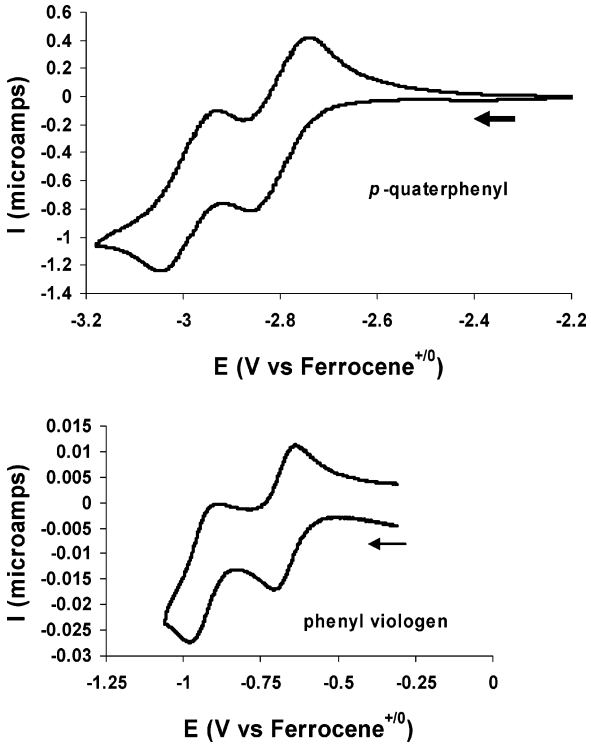

FIGURE 7. Cyclic voltammograms of *p*-quaterphenyl and $PV^{2+}[PF_6]_2$ as saturated solutions in THF.

it appears that a significant fraction of PV^0 can be substitutionally cocrystallized with *p*-quaterphenyl and the cocrystals maintain the crystal structure of *p*-quaterphenyl. However, the cocrystals displayed no significant electrical conductivity at room temperature.

Conclusions

Phenyl viologen has been synthesized, isolated, and characterized as a dication, radical cation, and neutral species. X-ray crystallography revealed a structural dichotomy between the dication and radical cation—twisted versus coplanar central rings—that had not been clearly demonstrated previously in viologens. The phenyl viologen radical cation exhibits behavior characteristic of many radical cations, including π-dimerization in the solid state and reversible π-dimerization in solution. The solid-state electrical conductivity of neutral phenyl viologen is about 3 orders of magnitude larger than that of the radical cation. A possible explanation for the higher conductivity of the neutral viologen is the fact that during hole transfer there is a significant geometric change between the radical cation and dication (the relevant species for conduction by the radical cation), whereas the neutral molecule and radical cation (the relevant species for conduction by neutral phenyl viologen) have similar structures.

Acknowledgment. We thank Jun Lang for assistance in acquiring the ESR spectrum and James Korp of the University of Houston for collecting single crystal X-ray diffraction data and assistance in solving the structures. Mass spectrometry was provided by the Washington University Mass Spectrometry Resource

(35) Hutchison, G. R.; Ratner, M. A.; Marks, T. J. *J. Am. Chem. Soc.* **2005**, *127*, 2339−2350.
(36) Meerholz, K.; Juergen, H. *J. Am. Chem. Soc.* **1989**, *111*, 2325−2326.

with support from the NIH National Center for Research Resources (Grant P41RR0954). Funding was provided by the National Science Foundation grant CHE 0133068, Research Corp. grant RI0697, and by the Department of Education (Graduate Assistance in Areas of National Need, Fund P200A000217).

Supporting Information Available: X-ray crystallographic information and data in CIF format for $PV^{2+}2Cl^{-}\cdot 2H_2O$ and $PV^{\bullet+}PF_6^{-}\cdot$pyridine are provided. This material is available free of charge via the Internet at http://pubs.acs.org.

JO050328G